

2004

## Macrophage tropism of HIV-1 depends on efficient cellular dNTP utilization by reverse transcriptase

Tracy L. Diamond

Mikhail Roshal

Varuni K. Jamburuthugoda  
*SUNY Geneseo*

Holly M. Reynolds

Aaron R. Merriam

*See next page for additional authors*

Follow this and additional works at: <https://knight scholar.geneseo.edu/biology>

---

### Recommended Citation

Diamond T.L., Roshal M., Jamburuthugoda V.K., Reynolds H.M., Merriam A.R., Lee K.Y., Balakrishnan M., Bambara R.A., Planelles V., Dewhurst S., Kim B. (2004) Macrophage tropism of HIV-1 depends on efficient cellular dNTP utilization by reverse transcriptase. *Journal of Biological Chemistry* 279: 51545-51553. doi: 10.1074/jbc.M408573200

This Article is brought to you for free and open access by the By Department at KnightScholar. It has been accepted for inclusion in Biology Faculty/Staff Works by an authorized administrator of KnightScholar. For more information, please contact [KnightScholar@geneseo.edu](mailto:KnightScholar@geneseo.edu).

---

**Authors**

Tracy L. Diamond, Mikhail Roshal, Varuni K. Jamburuthugoda, Holly M. Reynolds, Aaron R. Merriam, Kwi Y. Lee, Mini Balakrishnan, Robert A. Bambara, Vincente Planelles, Stephen Dewhurst, and Baek Kim

# Macrophage Tropism of HIV-1 Depends on Efficient Cellular dNTP Utilization by Reverse Transcriptase\*

Received for publication, July 28, 2004, and in revised form, September 22, 2004  
Published, JBC Papers in Press, September 26, 2004, DOI 10.1074/jbc.M408573200

Tracy L. Diamond<sup>‡§</sup>, Mikhail Roshal<sup>‡§</sup>, Varuni K. Jamburuthugoda<sup>¶</sup>, Holly M. Reynolds<sup>‡</sup>,  
Aaron R. Merriam<sup>‡</sup>, Kwi Y. Lee<sup>‡</sup>, Mini Balakrishnan<sup>¶</sup>, Robert A. Bambara<sup>¶||</sup>, Vicente Planelles<sup>\*\*</sup>,  
Stephen Dewhurst<sup>‡||</sup>, and Baek Kim<sup>‡ §§</sup>

From the <sup>‡</sup>Department of Microbiology and Immunology, <sup>¶</sup>Department of Biochemistry and Biophysics, and <sup>||</sup>Cancer Center, University of Rochester Medical Center, Rochester, New York 14642 and <sup>\*\*</sup>Department of Pathology, School of Medicine, University of Utah, Salt Lake City, Utah 84132

**Retroviruses utilize cellular dNTPs to perform proviral DNA synthesis in infected host cells. Unlike oncoretroviruses, which replicate in dividing cells, lentiviruses, such as human immunodeficiency virus type 1 (HIV-1) and simian immunodeficiency virus, are capable of efficiently replicating in non-dividing cells (terminally differentiated macrophages) as well as dividing cells (i.e. activated CD4+ T cells). In general, non-dividing cells are likely to have low cellular dNTP content compared with dividing cells. Here, by employing a novel assay for cellular dNTP content, we determined the dNTP concentrations in two HIV-1 target cells, macrophages and activated CD4+ T cells. We found that human macrophages contained 130–250-fold lower dNTP concentrations than activated human CD4+ T cells. Biochemical analysis revealed that, unlike oncoretroviral reverse transcriptases (RTs), lentiviral RTs efficiently synthesize DNA even in the presence of the low dNTP concentrations equivalent to those found in macrophages. In keeping with this observation, HIV-1 vectors containing mutant HIV-1 RTs, which kinetically mimic oncoretroviral RTs, failed to transduce human macrophages despite retaining normal infectivity for activated CD4+ T cells and other dividing cells. These results suggest that the ability of HIV-1 to infect macrophages, which is essential to establishing the early pathogenesis of HIV-1 infection, depends, at least in part, on enzymatic adaptation of HIV-1 RT to efficiently catalyze DNA synthesis in limited cellular dNTP substrate environments.**

Cellular dNTP levels serve as a biomarker for the replicative capacity of mammalian cells (for review, see Ref. 1). Consistent with this function, numerous studies have reported that dNTP contents in cancer cells and transformed cell lines are elevated 3–10-fold compared with normal cells and that dividing cells have higher dNTP contents than non-dividing cells (1–6). Cellular dNTP levels also fluctuate during the cell cycle and upon DNA damage, when replication and repair DNA synthesis lev-

els are altered (6–10). In addition, many viruses utilize cellular dNTPs to carry out their replicative cycle. These viruses include lentiviruses, such as the human and simian immunodeficiency viruses (HIV-1<sup>1</sup> and SIV), which are unique among retroviruses in their ability to infect both non-dividing cells, such as terminally differentiated macrophages (11), and dividing cells, such as activated CD4+ T cells. Changes in cell tropism between macrophages and T cells that occur during the course of lentiviral infection are closely related to immunological and clinical manifestations of lentivirus infection (i.e. CD4+ T cell decrease and AIDS). In contrast to lentiviruses, oncoretroviruses productively replicate only in dividing cells (11, 12). Therefore, it is intriguing to consider how lentiviral DNA polymerases may have evolved to replicate efficiently in quiescent cells (i.e. terminally differentiated/non-dividing macrophages) that presumably contain low levels of dNTPs.

In this study, we established a sensitive dNTP assay to measure dNTP concentrations in primary HIV-1-susceptible host cells. Biochemical analysis revealed that HIV-1 reverse transcriptase (RT) efficiently performs processive DNA synthesis under reaction conditions that contained dNTP concentrations equivalent to those found in macrophages. In contrast, oncoretroviral RTs were unable to efficiently polymerize under these conditions. Finally, we designed pseudotyped HIV-1 virus vectors that contained either wild-type RT or RTs with mutations that affected dNTP binding affinity. An analysis of reporter gene expression in vector-infected target cells revealed that the mutant constructs could transduce only actively dividing cells (cell lines, primary activated T cells), whereas the wild-type vectors could transduce both dividing and non-dividing (macrophage) host cells. Collectively, these data provide evidence that the unique ability of HIV-1 to infect non-dividing cells depends, at least in part, on the evolutionary adaptation of its reverse transcriptase to function under conditions of limiting dNTP availability.

## EXPERIMENTAL PROCEDURES

### Materials

Oligonucleotides were purchased from Integrated DNA Technologies. Hexahistidine-tagged p66/p66 RT homodimers derived from HIV-1 (HXB2) (13, 14) and SIV (SIVMNECL8) (15) or RT monomers of murine leukemia virus (MuLV) (16) were isolated from bacterial overexpression systems described in our previous studies. Avian myeloblastosis virus

\* This work was supported by National Institutes of Health Research Grants AI49781 (to B. K.), P01 MH64570 and S11 NS43499 (to S. D.), GM49573 (to R. A. B.), and AI49057 (to V. P.) and Training Grant T32 AI49815 (to M. R. and T. L. D.). The costs of publication of this article were defrayed in part by the payment of page charges. This article must therefore be hereby marked "advertisement" in accordance with 18 U.S.C. Section 1734 solely to indicate this fact.

§ Both authors contributed equally to this work.

§§ To whom correspondence should be addressed: Dept. of Microbiology and Immunology, University of Rochester, 601 Elmwood Ave., Box 672, Rochester, NY 14642. Tel.: 585-275-6916; Fax: 585-473-9573; E-mail: baek\_kim@urmc.rochester.edu.

<sup>1</sup> The abbreviations used are: HIV-1, human immunodeficiency virus type 1; SIV, simian immunodeficiency virus; T/P, template-primer complex; RT, reverse transcriptase; MuLV, murine leukemia virus; AMV, avian myeloblastosis virus; KF, Klenow fragment; GM-CSF, granulocyte-macrophage colony-stimulating factor; GFP, green fluorescent protein; MOI, multiplicity of infection.

(AMV) RT and Klenow fragment (KF) were purchased from Stratagene (La Jolla, CA) and New England Biolabs (Beverly, MA), respectively.

#### Single Nucleotide Incorporation Assay

Four different 19-mer DNA templates containing sequence variations (**N**) at the 5' end nucleotide (5'-**N**TGGCGCCCGAACAGGGAC-3') were individually annealed to an 18-mer DNA primer (5'-GTCCCTGTTCGGGCGCCA-3'), which was <sup>32</sup>P-labeled at its 5' end (template: primer, 4:1). The nucleotide at the 5' end of the primer determines the dNTP to be measured. The primer (160 pmol in 80  $\mu$ l) was labeled using 40 units of T4 polynucleotide kinase (New England Biolabs) with 80  $\mu$ Ci of [ $\alpha$ -<sup>32</sup>P]ATP (Amersham Biosciences) for 30 min at 37 °C. An additional 40 units of T4 polynucleotide kinase was added for an additional 30-min period of labeling. After heat inactivation (95 °C, 10 min), the labeled primer was split into four separate tubes annealed with each of the four 19-mer templates (160 pmol) with the addition of 10 $\times$  STE buffer (100 mM NaCl and 5 mM EDTA for final concentration) in a final volume of 50  $\mu$ l. The template/primer mixture was incubated for 10 min at 95 °C, 5 min at 55 °C, and 5 min at 22 °C and stored on ice until used.

The template/primer complexes (T/Ps) were extended using RT proteins in a standard dNTP assay reaction. Each assay reaction (20  $\mu$ l) contained 0.2 pmol of T/P (10 nM, primer concentration), 2  $\mu$ l of appropriate dNTPs (Amersham Biosciences) or extracted cellular dNTPs, 25 mM Tris-HCl, pH 8.0, 100 mM KCl, 2 mM dithiothreitol, 5 mM MgCl<sub>2</sub>, 5  $\mu$ M (dT)<sub>20</sub>, and 0.1 mg/ml bovine serum albumin (New England Biolabs). Reactions were initiated by adding excess RT proteins (60 nM) in relation to dNTP concentration (0.2–6.4 nM or 4–128 fmol in 20  $\mu$ l) and incubated at 37 °C for 5 min. Reactions were terminated with 10  $\mu$ l of 40 mM EDTA, 99% formamide. Reaction products were immediately denatured by incubating at 95 °C for 5 min, and 4  $\mu$ l of each 30  $\mu$ l of final reaction mixture was quantitated by phosphorimaging analysis (PerkinElmer Life Sciences) of 14% acrylamide-urea denaturing gels (SequaGel, National Diagnostics; model S2 sequencing gel electrophoresis apparatus, Labrepco). Note that in our purification protocol, ~30–60% of the purified RT protein was active as determined by our pre-steady-state kinetic assay using a similar 18-mer/40-mer primer/RNA template (17, 18). The reaction with less RT (10 nM), which is still a higher concentration than the highest dNTP concentration used (6.4 nM), gave a similar incorporation profile under the assay condition.

#### Standard Curves for Single Nucleotide Incorporation

The gels obtained from the incorporation assay (see Fig. 1A) were subjected to phosphorimaging analysis (see above). The percent of primer extension in each reaction was calculated by determining the ratios of extended *versus* total (extended and unextended) primers. Each signal for the extended products was normalized using the background signal in the control reactions incubated without RT (see Fig. 1C, lane C). The calculated percentage primer extension was plotted from triplicate reactions as a function of the dNTP quantity used, generating standard curves for all four dNTPs. The percentage primer extension determined in triplicate reactions containing extracted cellular dNTPs was then extrapolated to the standard curves to determine the dNTP contents present in the cellular samples.

#### Primer Extension by RT Proteins

The primer extension assay was modified from a previously described misincorporation assay (18). Briefly, an RNA T/P was prepared by annealing a 38-mer RNA (5'-AAGCUUGGCUGCAGAAUUGC-UAGCGGAAUUCGCGCG-3', Dharmacon Research) to the 17-mer A primer (5'-CGCGCCGAATTCCTCGT-3'; template:primer, 2.5:1, Invitrogen) <sup>32</sup>P-labeled at the 5' end by T4 polynucleotide kinase. Assay mixtures (20  $\mu$ l) contained 10 nM T/P, the RT protein concentrations specified in the legends to Fig. 2, A and B, and 4 dNTPs at concentrations indicated in the figure legends under the condition described in the dNTP assay above. Reactions were incubated at 37 °C for 5 min and terminated for analysis as described in the dNTP assay. Concentrations of RTs (*i.e.* 1 and 4 $\times$ ) and dNTPs (*i.e.* 4 and 0.04  $\mu$ M) used in each primer extension experiment were described in each figure legend. This reaction condition allows multiple rounds of primer extension. We also performed the single round primer extension. In this reaction, RTs were preincubated with the <sup>32</sup>P-labeled 17-mer/38-mer RNA template (10 nM), and the reaction was initiated by adding a mixture of dNTP (0.04  $\mu$ M) and a molar excess of cold T/P (1  $\mu$ M) for 3 min at 37 °C. For the trap control, RTs were preincubated with a mixture of the <sup>32</sup>P-labeled T/P and the cold T/P, and the reaction was initiated by adding dNTP (0.04  $\mu$ M). We also employed a 120-nucleotide-long RNA template annealed to a <sup>32</sup>P-labeled 20-mer primer (19). This T/P was also extended by differ-

ent concentrations of RTs and dNTP for 10 min at 37 °C (see Fig. 1D legend).

#### Steady-state Kinetic Analysis of dNTP Incorporation

The steady-state kinetic assay protocol described by Boosalis *et al.* (20) was modified to determine DNA polymerization efficiencies of DNA polymerases with the 18-mer/19-mer template/primers used in the dNTP assay (see above). Reaction conditions were the same as those described in the dNTP assay except for DNA polymerase concentrations (0.5–2 nM). For the analysis of dNTP incorporation kinetics, four different templates (5' template nucleotides T, C, G, or A for dATP, dGTP, dCTP, or dTTP incorporation, respectively) annealed to the <sup>32</sup>P-labeled 18-mer primer were used (see above). The amounts of RTs and incubation times were adjusted to yield an extension that was 30–60% of the total labeled primer (0.8 pmol) at the highest dNTP concentrations, and the reactions were repeated with eight decreasing concentrations of each dNTP. For HIV-1 RT, 5, 10, 20, 40, 80, 160, 320, and 720 nM dNTPs were used, and for MuLV RT, 1, 2, 4, 8, 16, 32, 64, and 128  $\mu$ M were used. We also measured the steady-state kinetic values using the processive reverse transcription with the 38-mer RNA annealed to the <sup>32</sup>P-labeled 17-mer. In this analysis, the different concentrations of all four dNTP mixtures were used. Products (single nucleotide-incorporated primer or all extended products) were resolved in 14% polyacrylamide-urea gel and quantitated by phosphorimaging analysis using the OptiQuant software (PerkinElmer Life Sciences). The  $k_{cat}$  and  $K_m$  values were determined from the Michaelis-Menten equation.

#### dNTP Extraction from Cells

The protocol for dNTP extraction from cells was similar to that described previously (21). Briefly, cell pellets ( $5 \times 10^4$ – $2 \times 10^6$  cells) were washed twice with 1 $\times$  Dulbecco's phosphate-buffered saline (Mediatech) and resuspended in 100  $\mu$ l of ice-cold 60% methanol. Samples were vortexed vigorously to lyse the cells and then heated at 95 °C for 3 min prior to centrifugation at 12,000  $\times g$  for 30 s. The supernatants were collected and completely vacuum-dried using a SpeedVac (Savant) with medium heat. The dried pellets were subsequently resuspended in dNTP buffer (50 mM Tris-HCl, pH 8.0, and 10 mM MgCl<sub>2</sub>; 100  $\mu$ l for  $1 \times 10^6$  HeLa cells and 10  $\mu$ l for  $1 \times 10^6$  primary cells), and usually 1–2  $\mu$ l of the extracted dNTP samples were used for each 20- $\mu$ l single nucleotide incorporation reaction (see above). The proper dilutions of the dNTP samples were prepared for the assay to make the primer extension values lie within the linear ranges of the dNTP incorporation (2–32% primer extension). The extracted dNTP samples were stored at –70 °C until used. Several different volumes of the extracted dNTP samples were also used to confirm the linearity of the primer extension. In addition, the dNTP samples were prepared from different cell numbers depending on the recovery efficiency of the primary cells from each blood sample (see below). However, the dNTP content of each cell type was normalized by pmol/ $1 \times 10^6$  (see Fig. 1F).

#### Isolation and Culture of Human T Cells and Monocyte-derived Macrophages

Human macrophages and CD4+ T cells were isolated from human buffy coats (Blood Research Institute) as described (22). Peripheral blood mononuclear cells were harvested from Ficoll density gradients (Lymphoprep, Axis-Shield PoC AS, Oslo, Norway), and monocytes were then purified using immunomagnetic selection with anti-CD14 antibody-conjugated magnetic beads following the manufacturer's recommendations (Miltenyi Biotec). CD4+ lymphocytes were isolated from monocyte-depleted buffy coats by immunomagnetic selection using anti-CD4 antibody-conjugated magnetic beads. The purified human monocytes were incubated in 10-cm dishes in RPMI 1640 medium (Mediatech) containing 20% human AB serum (Sigma) for 4 days in the presence of 5 ng/ml human recombinant GM-CSF (R&D Systems) and then incubated for an additional 3 days in the absence of GM-CSF to allow differentiation into macrophages. The purified resting T cells were maintained in RPMI 1640 medium supplemented with 10% autologous human serum, although activated T cells were propagated in RPMI 1640 medium supplemented with 10% autologous human serum and 5 ng/ml phytohemagglutinin (Sigma) for 24 h and then incubated in RPMI 1640 medium with 10% human serum and 5 ng/ml human recombinant interleukin 2 (Sigma) for 3 days. These cell preparations were to prepare for dNTP extracts and also for analysis of cell volumes using confocal microscopy.

#### Pseudotyped Virus Cloning and Preparation

pHCMV-VSVG envelope vector (23) and pD3-GFP transfer vector, which encodes the HIV-1 NL4-3 genome with the *eGFP* gene in place of

HIV-1 envelope, were used for preparing pseudotyped HIV-1. The V148I and Q151N mutations were cloned into pD3-GFP (pNL4-3-based) vector using the overlapping PCR with proper primers that were designed based on the pNL4-3 RT sequence. The created mutations were confirmed by sequencing with the 3305 primer (5'-GCACATAGGCTGTACTGTCC-3'), and correct *Swa*I relegation was confirmed with D3-GFP SEQ *Swa*I F (5'-CAGGCCATATCACCTAG-3') and D3-GFP SEQ *Swa*I R (5'-TCTAACTGGTACCATAAC-3') primers. 293FT cells (Invitrogen) were grown to ~90% confluency with Dulbecco's modified Eagle's medium, 10% fetal bovine serum, and 500 µg/ml G418 sulfate in T-175 flasks. The cells were transfected with 5 µg of envelope vector and 25 µg of transfer vector using Lipofectamine 2000 (Invitrogen) following the manufacturer's recommendations (in the absence of geneticin). Cells were split in half into two new T-175 flasks 16 h post-transfection. Supernatant was collected 48 and 72 h post-transfection and stored at 4 °C. Virus was harvested by ultracentrifugation at 22,000 rpm for 2 h at 4 °C with the Beckman SW 28 rotor. Virus was titrated by infection of HeLa cells<sup>2</sup> in the presence of polybrene, and the infection was monitored by fixation and flow cytometry analysis for GFP expression 48 h post-infection. p24 levels were also measured using the HIV-1 p24 antigen enzyme-linked immunosorbent assay test system (Beckman).

As a control, transfections were also performed in the absence of the pHCMV-VSVG vector, and this virus was titered on HeLa cells revealing no detectable GFP expression. In addition, controls were performed by pretreating HeLa cells for 2 h prior to and during infection with 0.5 mM cycloheximide, which is a general translation inhibitor. Cells were fixed and analyzed by flow cytometry 48 h post-infection. Results showed that very little protein was carried over with the pseudotyped virus preparations, as evidenced by <1% GFP-positive cells with plus cycloheximide infections compared with >20% GFP-positive cells in minus cycloheximide infections (data not shown).

#### Infection of Primary CD4<sup>+</sup> T Cells and Monocyte-derived Macrophage

T cells and macrophage were purified essentially as described above.

**T Cell Infections**—After 5 days of T cell stimulation with phytohemagglutinin and interleukin 2 (see above),  $2 \times 10^5$  stimulated T cells were infected in the presence of polybrene with a multiplicity of infection (MOI) of 100 based on HeLa cell titering. For QN virus infections, an MOI of 65 was used because of trouble generating high titer QN virus. These infections reflect the addition of viral stocks containing 200–300 ng of p24. Infected cells were incubated at 37 °C and 5% CO<sub>2</sub> in a 100-µl total volume. Two hours post-infection, 100 µl of RPMI 1640 medium with 10% heat-inactivated human AB serum and 4 ng/µl interleukin 2 was added, and infections were incubated for an additional 46 h. Cells were visualized and photographed by fluorescent microscopy to detect GFP fluorescence by infected cells. The percent of fixation was determined after cells were prepared for flow analysis by fixation with 0.5% formaldehyde.

**Macrophage Infections**—After the initial magnetic bead purification,  $2 \times 10^6$  CD14<sup>+</sup> cells/well were plated into 6-well plates and cultured in RPMI 1640 medium with 2% heat-inactivated human AB serum and 5 ng/ml GM-CSF for 48 h. This was followed by a 48-h incubation in RPMI 1640 medium with 20% heat-inactivated human AB serum and 5 ng/ml GM-CSF. Cells were then incubated for an additional 8 days in the absence of GM-CSF, with fresh medium added after the initial 4 days. Macrophages were infected with pseudotyped virus at an MOI of 40 based on HeLa cell titering and assuming  $1 \times 10^6$  cells/well in the presence of polybrene. These infections reflect the addition of viral stocks containing 80–130 ng of p24. Initial infections were in 250-µl volumes for the first 2 h at 37 °C and 5% CO<sub>2</sub> followed by the addition of 2 ml of RPMI 1640 medium with 20% heat-inactivated human AB serum. Incubations were continued for up to 6 days, and cells were periodically examined for GFP fluorescence by fluorescent microscopy. Cells were fixed in 0.5% formaldehyde after disassociation from the plates by 30 min of incubation with 2 mM EDTA and gentle scraping. The percent of infection was determined by flow cytometry.

## RESULTS AND DISCUSSION

**Determination of dNTP Levels in HIV-1 Target Cells, Human Macrophages, and Resting or Activated CD4<sup>+</sup> T Cells**—First, we established a highly sensitive enzymatic dNTP assay that

allowed us to measure the dNTP contents of primary and non-dividing cells such as macrophages. For the enzymatic measurement of each dNTP contained in a mixture of four different dNTPs, we designed a <sup>32</sup>P-labeled 18-mer primer that could anneal to any of four different 19-mer DNA templates (see "Experimental Procedures"). Because these dNTP assay T/Ps contain only one of the four possible nucleotides at the 5' protruding end of the template, DNA polymerases can incorporate only the complementary dNTP onto each of the four T/Ps. Using the specific T/Ps, we found that HIV-1 RT efficiently performed single nucleotide incorporation, even at very low dNTP concentrations, compared with KF of *Escherichia coli* DNA polymerase I (data not shown) and MuLV RT (see below). When 200 fmol of T/Ps were extended by HIV-1 RT (60 nM) in the presence of different amounts of the individual dNTPs for 5 min at 37 °C, 19-mer extended products were generated. As shown in Fig. 1A, incorporation of dCTP and dTTP was detected at concentrations as low as 4 fmol, which extended ~2% of the primers. Similar profiles were seen with dGTP and dATP (data not shown). The percent of primer extension in each reaction was then calculated to generate standard curves for incorporation of each dNTP onto the appropriate template/primer (Fig. 1B, dTTP and dGTP). No detectable primer extension was observed in control reactions lacking either HIV-1 RT or the required dNTP (Fig. 1C, lane C). The single nucleotide primer extension reaction for each of the four dNTPs was found to be linear for dNTP quantities between 4 and 128 fmol (0.2–6.4 nM), as shown in the standard curve with dTTP and dGTP (Fig. 1B) as well as with dATP and dCTP (data not shown). The linear dNTP incorporation appeared to be affected at higher dNTP amounts in some cases (see 128 fmol dTTP in Fig. 1B) because the observed primer extension levels with 128 fmol of dNTPs (55–60%) were lower than expected (64% at 128 fmol). Therefore, the upper dNTP limit of the assay should be 128 fmol. This suggested that the dNTP content measurement with the dNTP samples extracted from cells should be performed within the linear dNTP ranges (4–64 fmol of dNTP or 2–32% of primer extension). The minimum detection of the dNTP content in this HIV-1 RT-based assay (4 fmol) is 25- and 500-fold more sensitive than the KF (0.1 pmol) (21) and high pressure liquid chromatography-based assays (>2 pmol) (25–28), respectively, that have been used previously for dNTP content measurement.

These reactions contained excess HIV-1 RT in relation to substrates, allowing depletion of provided dNTPs within the linear range, as shown in Fig. 1. This explanation is evidenced by the following: 1) the assay was performed at 10 and 20 min, and no additional primer extension compared with the 5 min standard reaction was observed (data not shown); and 2) the assay showed a 1:1 correlation between the amount of extended primer and the amount of dNTPs included in the reaction, particularly at the low dNTP amount (e.g. adding 4 fmol of dCTP resulted in 2% primer extension).

dNTP samples obtained from cells contained all four dNTPs as well as structurally related rNTPs, which may be present in cells with concentrations 200–1000-fold higher than the dNTPs (1). Thus, it is conceivable that an enzymatic dNTP assay might be influenced by the presence of such a vast excess of rNTPs. This is unlikely in the case of HIV-1 RT, which has been shown to incorporate rNTPs very inefficiently (i.e. only when their concentration is at least 0.5 mM) (29). Nonetheless, we tested our assay by adding rNTPs at a concentration 10,000-fold higher than the highest dNTP concentration in the linear range of the assay, and rNTP incorporation was not detected (Fig. 1C). A second potential concern with using a primer extension reaction based on the HIV-1 RT is that this enzyme

<sup>2</sup> Obtained through the AIDS Research and Reference Reagent Program, Division of AIDS, NIAID, National Institutes of Health from Dr. Richard Axel (24).

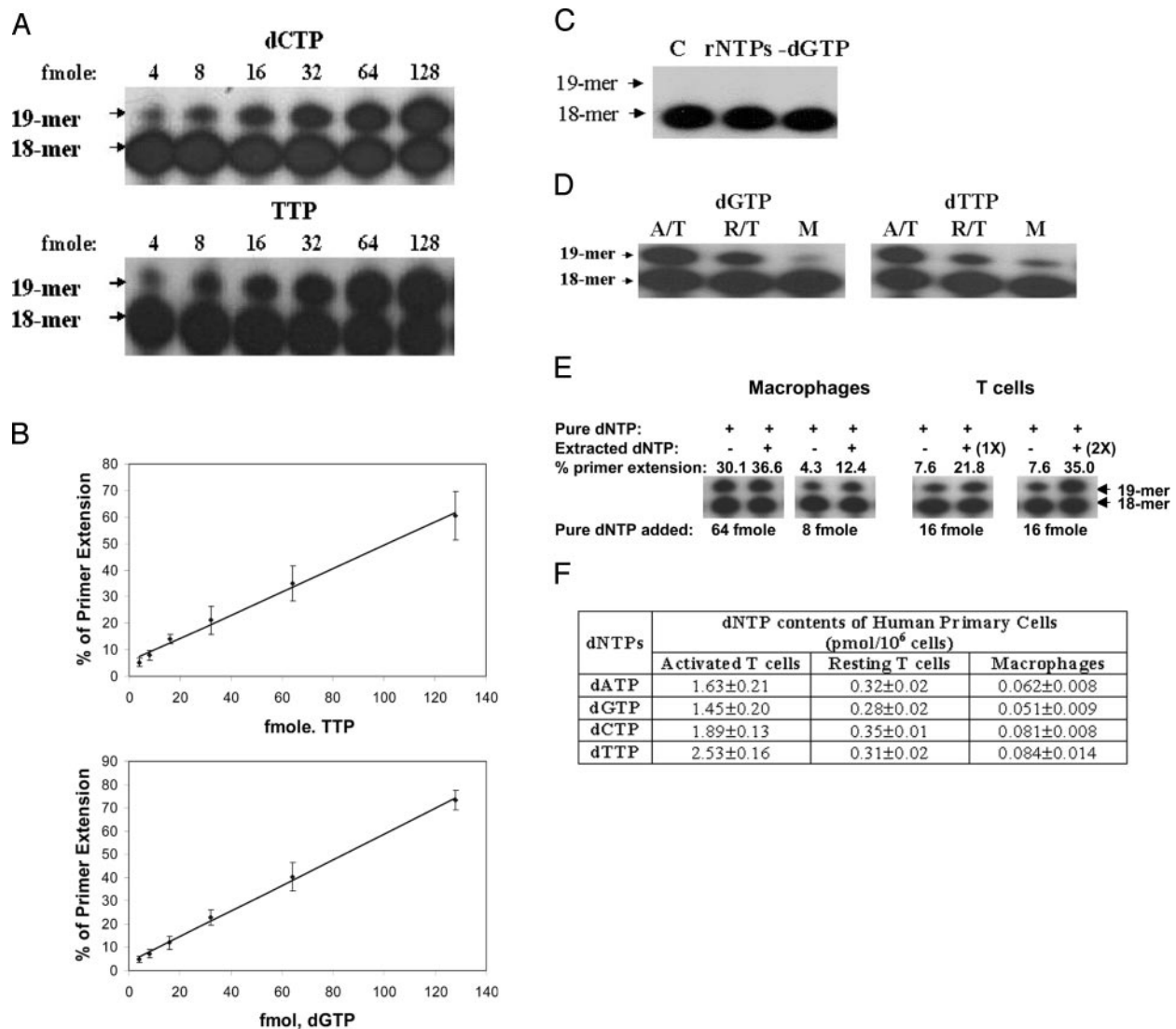


**FIG. 1. Primary cell dNTP content determination by the HIV-1 RT-based dNTP assay.** *A*, dCTP and dTTP incorporation by HIV-1 RT (60 nM) was measured using the dCTP-specific template/primer pair (200 fmol) in the presence of different amounts of dCTP. *B*, standard curve for the incorporation of dTTP and dGTP onto the dTTP- and dGTP-specific template/primer pairs. The percent of primer extension in each reaction was plotted after background normalization (see "Experimental Procedures"). Each data point was calculated from three independent reactions; error bars denote the standard deviation from the mean. *C*, incorporation of incorrect dNTPs and rNTPs. The G-specific template/primer pair was incubated with HIV-1 RT (60 nM) and 50  $\mu$ M rNTP or a mixture of three incorrect dNTPs ( $-dGTP$ ), which corresponds to a mixture that contained 0.5  $\mu$ M each dTTP, dCTP, and dATP. *D*, dNTP samples were isolated from human activated (A/T) or resting (R/T) CD4<sup>+</sup> T cells or CD14<sup>+</sup> macrophages (M). dNTP samples contained in 1 (T cells) to 2 (macrophages)  $\times 10^5$  cells were used for each assay reaction using dGTP- or dTTP-specific template/primer pairs. *E*, effect of other chemicals contained in the extracted dNTP samples. The dNTP assay was performed with either pure dNTP or mixtures of pure and extracted dNTPs. The amounts of the pure dNTPs used in the reactions are shown below the gels, and 1 (T cells) or 2 (macrophages)  $\mu$ l of the cellular dNTP sample was used. The percent of primer extension in each reaction is also shown. Two different amounts of the T cell dNTP sample, 1 and 2 $\times$ , were used. The results for all template/primer pairs with the extracted dNTP samples are summarized in *F*. dNTP values shown represent mean values calculated from three independent experiments performed in triplicate; standard deviations are shown for each value. All reactions were performed as described under "Experimental Procedures," and products were analyzed by electrophoresis through 14% denaturing polyacrylamide gels followed by phosphorimaging analysis (see "Experimental Procedures").

is known to be error-prone (*i.e.* capable of incorporating "incorrect" dNTPs) (30, 31). We therefore tested whether incorrect dNTPs could be incorporated under the assay conditions used. For this test, the dGTP-specific template/primer pair was extended in the presence of a mixture of dATP, dCTP, and dTTP (0.5  $\mu$ M each), the three incorrect dNTPs; this incorrect dNTP concentration is  $\sim$ 100-fold higher than the highest correct dNTP concentrations that showed linear incorporation under these assay conditions (6.4 nM dGTP). As shown in Fig. 1C, no incorporation of incorrect dNTPs was observed even at this artificially high concentration of incorrect dNTPs. In fact, HIV-1 RT needs  $\sim$ 200  $\mu$ M incorrect dNTPs to carry out misincorporation under similar reaction conditions (32, 33). Therefore, incorrect dNTPs and rNTPs present in cellular dNTP

samples should not interfere with the determination of individual dNTP levels under the assay conditions established.

We used the HIV-1 RT-based assay to examine dNTP levels in the major primary target cells for HIV-1 (*i.e.* human monocyte-derived macrophages and activated or resting CD4<sup>+</sup> T cells). For this analysis, dNTPs were extracted from these primary cells (see "Experimental Procedures"), and the extracted dNTP samples with the proper dilutions were used as the dNTP source in single nucleotide extension assays with each of the four T/Ps. As shown in Fig. 1, D and F, human macrophages were found to contain  $\sim$ 4- and  $\sim$ 20-fold less dNTPs than resting and activated T cells, respectively. The dNTP content of T cells determined in this assay was found to be similar to that previously determined by the KF based assay

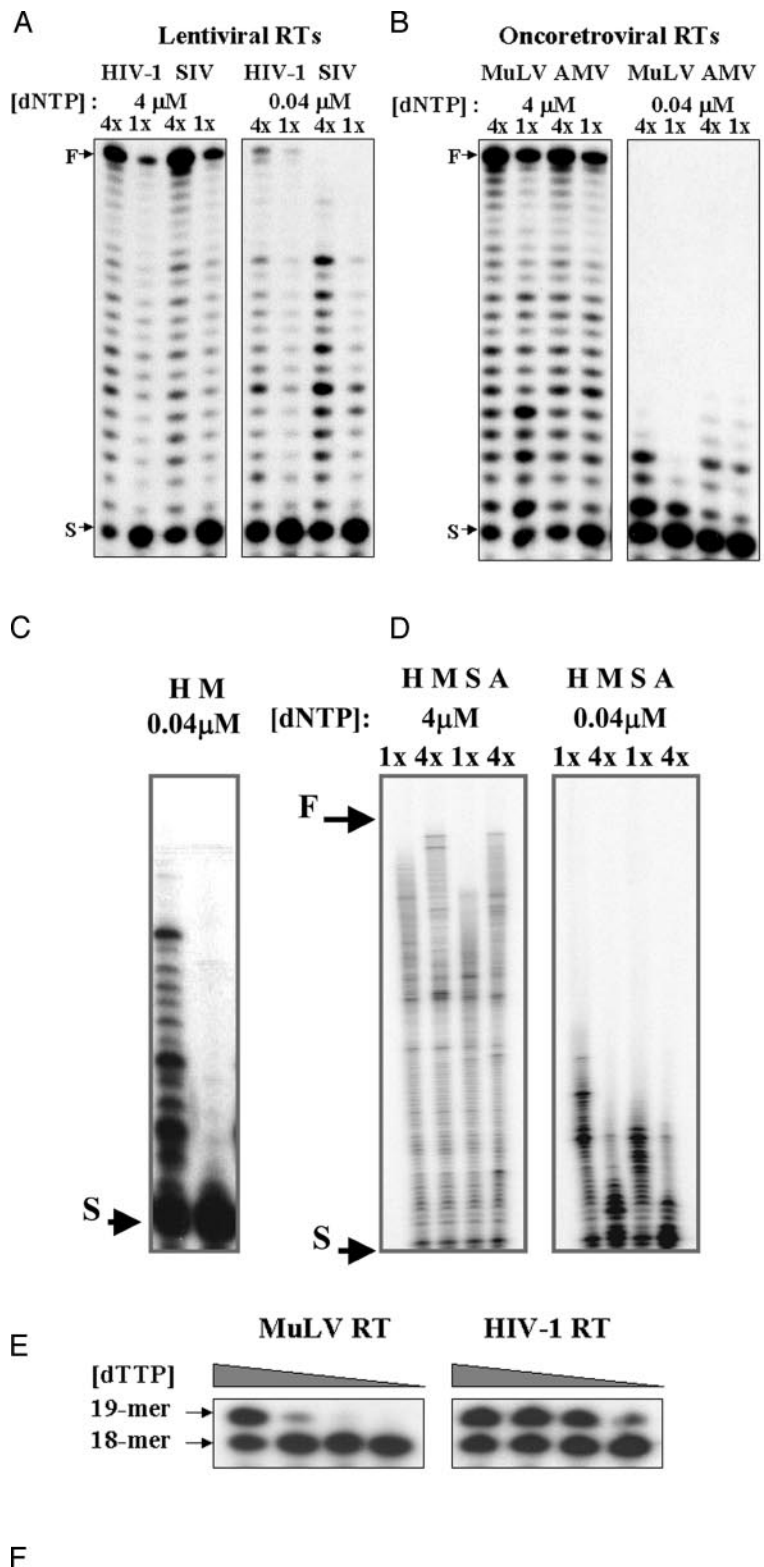
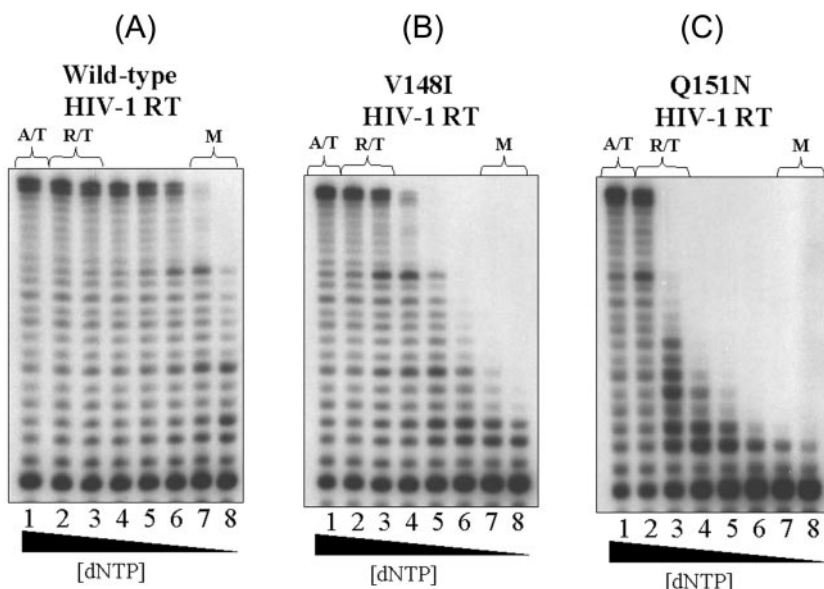


**FIG. 2. Comparison of reverse transcription capability of lentiviral and oncoretroviral RTs at different dNTP concentrations.** A  $^{32}$ P-labeled 17-mer primer (S) was annealed to a 38-mer RNA template and then extended by two lentiviral RTs (A), HIV-1 and SIV RTs, and two oncoretroviral RTs (B), MuLV and AMV RTs, in reactions containing each dNTP at 4  $\mu$ M. Two different input levels of RT activity were used in these reactions (1 $\times$  and 4 $\times$ , as indicated). The RT reactions were repeated with these same two reverse transcription activities (4 $\times$  and 1 $\times$ ) in reactions that contained each dNTP 0.04  $\mu$ M; the fully extended primer is 38 nucleotides long (lane F). 4 $\times$  concentrations of RTs are as follows: HIV-1 RT, 3.2 nM; SIV RT, 6 nM; MuLV RT, 0.5 nM; AMV RT, 2.25 nM. The same T/P used in A and B was extended by HIV-1 (3.2 nM) and MuLV RTs (0.5 nM) under the condition allowing a single round of primer extension at 0.04  $\mu$ M dNTP (C). A  $^{32}$ P-labeled 20-mer primer (S) annealed to a 120-nt-long RNA template encoding HIV-1 RT genome (D) was extended at 4 and 0.04  $\mu$ M dNTP by the four RTs under the same condition used in A and B. The 2 $\times$  concentration was used for the two lentiviral RTs (H, 6.4 nM HIV-1 RT; S, 12 nM SIV RT), whereas the 8 $\times$  concentration was used for the two oncoretroviral RTs (M, 4 nM MuLV RT; A, 9 nM AMV RT). E, dNTP concentration-dependent single nucleotide incorporation by MuLV and HIV-1 RTs was determined on the 18-mer/19-mer assay T/Ps. The single nucleotide incorporation activity of these two DNA polymerases at different dNTP concentrations was analyzed using the T-specific template/primer pair (10 nM) in the presence of decreasing dTTP concentrations (50, 5, 0.5, and 0.05  $\mu$ M). The 18-mer and 19-mer primers indicate unextended and extended primers, respectively. Polymerase concentrations showing  $\sim$ 60% primer extension on this template/primer pair at 50  $\mu$ M dTTP are 1 nM MuLV RT and 0.8 nM HIV-1 RT. F, steady-state kinetic analysis of the two DNA polymerases with the four 18-mer/19-mer T/Ps is shown (see "Experimental Procedures"). Results are from experiments performed in triplicate with standard deviations.

dNTPs	MuLV RT		HIV-1 RT	
	$K_M$ ( $\mu$ M)	$k_{cat}$ ( $\text{min}^{-1}$ )	$K_M$ ( $\mu$ M)	$k_{cat}$ ( $\text{min}^{-1}$ )
dGTP	4.96 $\pm$ 0.38	0.32 $\pm$ 0.09	0.0328 $\pm$ 0.007	0.60 $\pm$ 0.03
dATP	29.2 $\pm$ 6.3	0.38 $\pm$ 0.09	0.0641 $\pm$ 0.0003	0.45 $\pm$ 0.04
dTTP	27.5 $\pm$ 6.1	0.43 $\pm$ 0.05	0.0655 $\pm$ 0.025	0.43 $\pm$ 0.07
dCTP	6.52 $\pm$ 1.54	0.42 $\pm$ 0.06	0.1280 $\pm$ 0.023	0.35 $\pm$ 0.05

**FIG. 3. dNTP dependence of HIV-1 Wild-type (A), V148I (B), and Q151N (C) RT mutants during multiple round polymerization.** The  $^{32}\text{P}$ -labeled 17-mer primer annealed to the 38-mer RNA template was extended by equivalent activities of the three RTs (as determined by analysis of enzymatic activity under reaction conditions that contained  $5\ \mu\text{M}$  each dNTP). Reactions were then conducted with decreasing equimolar concentrations of all four dNTPs and were analyzed on a 14% denaturing polyacrylamide gel. Lanes 1–8 correspond to 5, 2.5, 1, 0.5, 0.25, 0.1, 0.05, and  $0.025\ \mu\text{M}$  concentrations of all four dNTPs, respectively. Reactions performed at concentrations that represent those found in activated (A/T) and resting (R/T) T cells and macrophages (M) are marked.



(21). We also confirmed the dNTP content of human resting CD4<sup>+</sup> T cells using the KF-based assay previously established, but this assay required 10–20-fold more cells per assay because of the higher assay sensitivity limit (0.1 pmol).

Next, we tested the nonspecific inhibition of the HIV-1 RT activity by other chemicals co-extracted with cellular dNTPs under the dNTP assay condition. For this test, we performed the dNTP assay with either pure dNTP (64 or 8 fmol of dTTP for the macrophage samples and 16 fmol of dGTP for the T cell samples; Fig. 1E) or mixtures of pure dNTP and the extracted dNTP samples used in Fig. 1D. As shown in Fig. 1E, even with  $2\ \mu\text{l}$  of the macrophage extract sample, which contains 16.8 fmol of dTTP (Fig. 1F), the primer extension with 64 fmol of dTTP was not reduced. Rather, compared with the reaction with only pure dTTP (30.1%), a slight increase ( $\sim 7\%$ ) was observed in the reaction with this mixture. This increase likely resulted from the additional incorporation of dTTP contained in the macrophages sample (16.8 fmol), which should have given  $\sim 8\%$  primer extension. More obviously, as shown in Fig. 1E, the reaction with the mixture of 8 fmol of pure TTP (theoretically giving 4% primer extension) and  $2\ \mu\text{l}$  of the macrophage sample (16.8 fmol of TTP giving 8.4% primer extension) showed 12.4% primer extension, whereas the reaction with only 8 fmol of pure dTTP showed the expected 4.3% primer extension. The 8.1% primer extension increase in the reaction with this mixture likely resulted from the incorporation of the 16.8 fmol of dTTP (Fig. 1F) contained in the  $2\ \mu\text{l}$  of the macrophage sample. As shown in Fig. 1E, the additive primer extension was also observed in the reactions with the mixtures of pure dGTP (16 fmol, 7.6% primer extension) and the resting T cell samples containing 28 ( $1\times$  and  $1\ \mu\text{l}$ ) or 56 ( $2\times$  and  $2\ \mu\text{l}$ ) fmol of dGTP (giving additional 14.2 and 27.4% primer extensions, respectively) as well as activated T cells (data not shown). In addition, the expected primer extension increases were seen when the pure dNTPs (Fig. 1E) were added into the reactions with only extracted samples (Fig. 1, D and F). For example, the reaction with a mixture of 16 fmol of pure dGTP, which gave 7.6% primer extension, and the resting T cell sample ( $1\times$  and  $1\ \mu\text{l}$ ) containing 28 fmol dGTP (theoretically giving 14% primer extension (Fig. 1F) or actually giving 13.1% primer extension (Fig. 1D)) showed 21.8% primer extension (Fig. 1E). This indicates that the 16 fmol of pure dGTP, which produces 8% primer extension, contributed to 7.8 (theoretical) to 8.7% (actual calculated) primer extension increases. Therefore, this

result supports the notion that the incorporation of the pure dGTP was not significantly affected by the addition of the extracted sample ( $2\ \mu\text{l}$ ). Similar cases can be observed with the  $2\times$  T cell samples as well as with the macrophage samples, when the data shown in Fig. 1F (with only extracted dNTP sample) and Fig. 1E (with mixtures of pure and extracted dNTPs) are compared. We also performed the poly(rA)/oligo(dT)-based RT assay measuring the  $[\text{H}]\text{TTP}$  incorporation in the presence or absence of  $2\ \mu\text{l}$  of cellular dNTPs samples, and in this experiment also we did not observe any reduction of the  $[\text{H}]\text{TTP}$  incorporation by the cellular dNTP samples (macrophages, T cells, and HeLa cells; data not shown). Therefore, the data shown in Fig. 1E, together with the observations from the  $[\text{H}]\text{TTP}$  incorporation RT assay, clearly demonstrate that HIV-1 RT activity is either not affected or is only slightly affected by the inhibitory effects of other chemicals contained in the extracted dNTP samples. In fact, the protocol employed in this assay has been established previously for similar types of enzymatic dNTP assays (21). We also used several different volumes of the extracted dNTP samples for the dNTP measurements, and with these varied amounts of the samples, we observed the expected linear changes in the percent of primer extension. These data allow us to use 1) the percentages of the primer extension with the extracted cellular dNTP samples and 2) the dNTP standard curves shown in Fig. 1B for determining the dNTP content in each extracted sample.

Because there is no compartmentalization of cellular dNTPs between the nucleus and cytoplasm (1), the average cell volumes have been used to calculate the cellular dNTP concentrations. The dNTP concentrations in these three human primary cells were then calculated by taking into account the volumes of these cell types. The cell volumes of human macrophages and resting and activated CD4<sup>+</sup> T cells were calculated using confocal microscopy and found to be 2660, 186, and  $320\ \mu\text{m}^3$ , respectively, which are similar to previously published estimates (34–36). Therefore, the calculated dNTP concentrations in human macrophages are  $\sim 130$ – $250$ -fold lower ( $\sim 0.026\ \mu\text{M}$ ) than in resting and activated CD4<sup>+</sup> T cells (3.4 and  $6.2\ \mu\text{M}$ , respectively; Fig. 1D).

**Reverse Transcription Activity of Retroviral RTs at dNTP Concentrations Found in T Cells and Macrophages**—Lentiviruses differ from oncoretroviruses in their ability to infect non-dividing cells such as macrophages (11, 12). HIV-1 infection of terminally differentiated, tissue-resident cells of monocytic lineage may be especially important during viral trans-

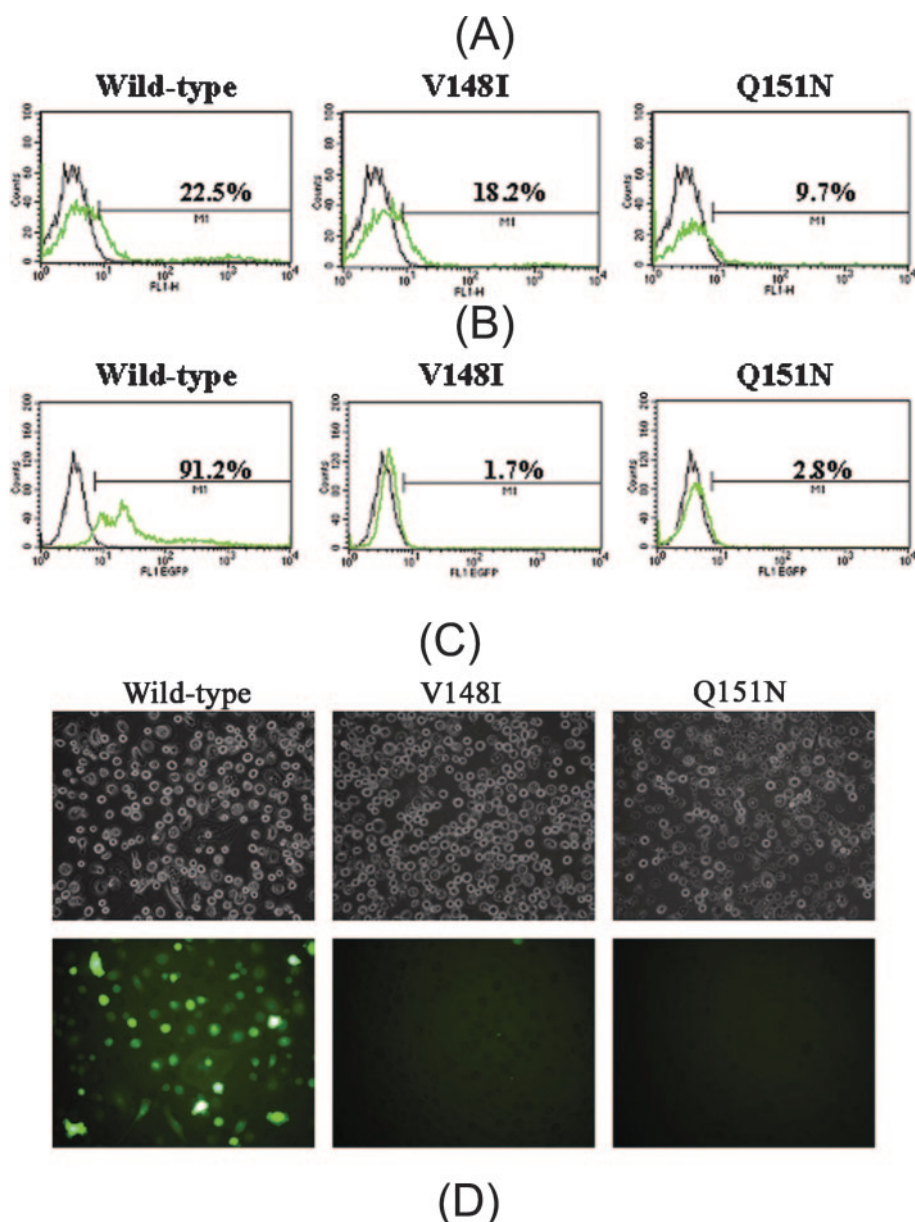


FIG. 4. Transduction of primary human cells by pseudotyped lentivirus vectors containing wild-type, V148I, or Q151N RTs. Primary human cells were infected with eGFP-encoding lentivirus vectors containing the indicated RT variants (*Wild-type*, *V148I*, *Q151N*). T cells were fixed 48 h post-infection with 0.5% formaldehyde, and macrophages were fixed 120 h post-infection in 0.5% formaldehyde after treatment with 2 mM EDTA and gentle scraping. Flow cytometric analysis of eGFP expression in transduced CD4+ T cells (A) and macrophages (B) from one representative experiment are shown. The negative control (mock) infections are shown in *black*, whereas results from vector-transduced cells are depicted by the *green* histograms. Total cells were gated on the basis of physical parameters (forward and side scatter), and the percent GFP-positive cells was determined after gating parameters were set such that the percent GFP-positive cells in the negative control cells was 1%. C, representative images of macrophages 120 h post-infection are shown. Fluorescent images are shown (*upper panels*) with corresponding bright field images (*lower panels*); images were taken at  $\times 14$  magnification. A summary of flow cytometric results from one experiment performed in triplicate is shown in D.

mission and early replication events (37, 38). In contrast, like other RNA tumor viruses, MuLV (11) and AMV (39, 40) infection requires cell proliferation. However, AMV infection of chicken embryo-derived macrophages has been described only when these cells were actively dividing as confirmed by [ $^3$ H]thymidine incorporation and mitotic index (39, 40). Because the calculated dNTP concentration present in primary macrophages is very low ( $\sim 0.03 \mu\text{M}$ ), we performed a series of experiments employing various substrates and reaction condi-

tions to examine whether lentiviral (HIV-1 and SIV) and oncoretroviral (MuLV and AMV) RTs were able to execute processive DNA synthesis under reaction conditions that contained dNTP concentrations present in macrophages ( $0.04 \mu\text{M}$ ) or T cells ( $4 \mu\text{M}$ ) (Fig. 2).

First, a 17-mer primer annealed to a 38-mer RNA template was employed for monitoring reverse transcription. The RT enzymes being compared were then added at two different quantities (4 and 1 $\times$ ); as expected, these different levels of

<sup>a</sup> Multiplicity of infection based on titering on HeLa cells and infection of  $2 \times 10^5$  stimulated T-cells or  $1 \times 10^6$  macrophages.  
<sup>b</sup> Due to less efficient production of high titer virus with the QN mutation, a lower MOI was added for these infections. Extrapolated data for the same MOI used for WT and VI is shown in parentheses.

input enzyme resulted in an ~4-fold difference in the amount of fully extended primer (Fig. 2, A and B, lane F) at the dNTP concentration present in T cells ( $4 \mu\text{M}$ ). However, when the primer extension was performed in the presence of  $0.04 \mu\text{M}$  of each dNTP (*i.e.* the concentration present in macrophages), the two lentiviral RTs still maintained efficient DNA synthesis capabilities (Fig. 2A), whereas the two oncoretroviral RTs showed a dramatic reduction in their ability to conduct multiple rounds of DNA synthesis (Fig. 2B). Note that slightly more reverse transcription activity was added for reactions with MuLV RT to demonstrate that even with more DNA polymerase activity, MuLV RT did not extend the primer efficiently at  $0.04 \mu\text{M}$  dNTP. In addition, reactions were performed with HIV-1 and MuLV RTs for longer incubation times with  $0.04 \mu\text{M}$  dNTPs, and we observed further extension of the primer, implying that all substrate dNTPs were not depleted under these reaction conditions (data not shown). Therefore, the low levels of primer extension seen for MuLV RT at  $0.04 \mu\text{M}$  dNTP concentrations are not because of dNTP depletion.

Second, we examined the effect of dNTP concentration on the DNA polymerization of HIV-1 and MuLV RTs under the condition allowing a single round of primer extension. This analysis employed the same reaction condition as described in the legend for Fig. 2, A and B (multiple round primer extension), except using a trap that is a 100-fold molar excess of cold T/P. In this reaction, HIV-1 and MuLV RTs ( $4\times$  concentration) were preincubated with the  $^{32}\text{P}$ -labeled 17-mer primer annealed to the 38-mer RNA template, and then the RT reaction was initiated by adding a mixture of  $0.04 \mu\text{M}$  dNTP and the cold T/P trap. As shown in Fig. 2C, under this single round extension condition with  $0.04 \mu\text{M}$  dNTP, less primer extension was observed in the reaction with HIV-1 RT than with the multiple round primer extension by HIV-1 RT at  $0.04 \mu\text{M}$  (Fig. 2A). We also confirmed the single round primer extension by initiating the reaction containing RTs preincubated with both the cold trap and the  $^{32}\text{P}$ -labeled T/P by adding  $0.04 \mu\text{M}$  dNTPs. In this trap control, no primer extension was observed (data not shown), indicating that the data shown in Fig. 2C was generated under the single round primer extension condition. Indeed, as shown in Fig. 2C, HIV-1 RT was still able to perform the single round of the primer extension very efficiently at  $0.04 \mu\text{M}$  dNTP compared with MuLV RT, which did not incorporate more than one nucleotide. This confirms the dNTP utilization discrepancy between HIV-1 RT and MuLV RT at low dNTP concentrations.

Third, we also used the multiple round primer extension assay using a 120-nucleotide-long HIV-1 RNA template annealed to a  $^{32}\text{P}$ -labeled 20-mer primer (19). As shown in Fig. 2D, even with a 4-fold greater RT activity ( $8\times$ ; see  $4 \mu\text{M}$  dNTP reactions), the two oncoretroviral RTs (M, MuLV RT; A, AMV RT) showed significant low primer extension at  $0.04 \mu\text{M}$  dNTP, compared with the two lentiviral RTs (H, HIV-1 RT; S, SIV RT). This result is similar to those described in Fig. 1, B and C, using the 38-mer RNA template.

Last, we examined the effect of the dNTP concentration on the DNA synthesis kinetics of HIV-1 and MuLV RTs, comparing the steady-state kinetic parameters of these two RTs measured by a single nucleotide incorporation assay. This experiment was performed on the 18-mer/19-mer template/primer used for the dNTP assay but with more limiting RT concentrations than those used in Fig. 1A. Fig. 2E demonstrates the qualitative difference between HIV-1 and MuLV RT in the single nucleotide incorporation with varying dNTP concentrations. Initially, RT activity showing ~60% extension at  $50 \mu\text{M}$  dTTP under the standard reaction condition described in Fig. 2A was determined, and then the same reactions were repeated at three different lower dTTP concentrations ( $5$ ,  $0.5$ , and  $0.05 \mu\text{M}$ ). Indeed, as shown in Fig. 2E,

at lower dNTP concentrations, HIV-1 RT was able to polymerize single nucleotide incorporation much more efficiently than MuLV RT. Next, the steady-state kinetic parameters  $K_m$  and  $k_{\text{cat}}$  were calculated under similar reaction conditions but with lower RT activity than was used in Fig. 2E. As seen in Fig. 2F, the  $k_{\text{cat}}$  values for the two enzymes with the four dNTPs did not vary greatly, whereas there was a large increase in the  $K_m$  values for the MuLV RT as compared with HIV-1 RT. Furthermore, in processive DNA synthesis assays similar to Fig. 2, A and B, we also found that the  $K_m$  values of MuLV and AMV RTs were 23- and 20-fold higher than that of HIV-1 RT, respectively, with similar  $k_{\text{cat}}$  values between these RTs (data not shown). Therefore, these  $K_m$  differences confirm that at lower dNTP concentrations, HIV-1 RT is able to polymerize DNA more efficiently than MuLV RT.

The data obtained from the various assays shown in Fig. 2 clearly suggest that the lentiviral RTs have evolved to efficiently catalyze DNA polymerization even at very low dNTP concentrations (such as those found in primary macrophages). In contrast, the oncoretroviral RTs may have adapted to efficiently catalyze DNA synthesis only at the much higher dNTP concentrations (*i.e.*  $4 \mu\text{M}$ ) that are present in actively dividing cells.

**HIV-1 Replication in Human Primary Target Cells with Different dNTP Concentrations**—To further examine the relationship between cellular dNTP content and retroviral replication, we took advantage of two mutated derivatives of the HIV-1 RT, V148I and Q151N, that had recently been shown by pre-steady-state kinetic analysis to have severely reduced dNTP binding affinity ( $k_d$ , 25.6- and 234.2-fold respectively) compared with wild-type HIV-1 RT, even though these mutants possess wild-type levels of catalysis ( $k_{\text{pol}}$ ) (14, 17). As seen in Fig. 3, we examined the dNTP concentration dependence of processive DNA polymerization by these mutant RTs as compared with wild-type RT. Each of the RTs exhibited similar levels of activity in reactions that contained high dNTP concentrations (*i.e.*  $5 \mu\text{M}$  in Fig. 3), which is supported by their identical  $k_{\text{pol}}$  values. The wild-type HIV-1 RT was also able to efficiently polymerize DNA even at the low dNTP concentrations found in macrophages (Fig. 3A). However, similar to the two oncoretroviral RTs tested above (Fig. 2B), the two mutant HIV-1 RTs were significantly diminished in their ability to conduct processive DNA synthesis at the low dNTP concentrations found in macrophages. The dNTP binding to the active site of the mutant RTs likely becomes a rate-limiting step during the steady-state primer extension reaction at low dNTP concentrations. Overall DNA polymerization capability at the dNTP concentrations found in macrophages is greatest for wild-type RT, followed by V148I RT and then Q151N RT, which displayed the most significant decrease in dNTP binding affinity (14, 17). Our kinetic analysis demonstrated that, like these HIV-1 dNTP binding mutants, MuLV RT also has a 40–75-fold higher  $k_d$  than wild-type HIV-1 (data not shown). Basically, these HIV-1 RT dNTP-binding mutants kinetically mimic MuLV (Fig. 2B).

Next, to examine the effect of RT dNTP binding affinity on lentiviral replication in primary cells, we generated pseudotyped HIV-1 vectors that contained an eGFP reporter cassette and that were isogenic except for the previously defined RT mutations (*i.e.* wild type, V148I, and Q151N). The pseudotyped particles were titered on HeLa cells, and then equivalent MOIs were used to infect primary human T cells and macrophages. As seen in Fig. 4, A and D, all three vectors had similar abilities to transduce activated human T cells and transformed cell lines (*i.e.* HeLa cells) containing high cellular dNTP concentrations, which is consistent with the efficient polymerization capability of wild-type RTs and these mutant HIV-1 RTs at high concentrations (Fig. 2C) and their similar  $k_{\text{cat}}$  values (Fig. 2D). In contrast, the

vectors containing the V148I and Q151N RT mutants were greatly diminished in their ability to transduce primary macrophages even with higher MOI infections (Fig. 4, B–D). Therefore, this reflects the enzymatic inability of these mutant RTs to synthesize DNA at low dNTP concentrations and suggests that the dNTP binding affinity of lentiviral RTs is a key contributor to viral replication in macrophages.

In summary, using both biochemical and virological analyses, we were able to investigate the relationship between cellular dNTP pools, RT binding affinity for dNTPs, and viral replication in non-dividing host primary cells that contain limiting dNTP concentrations. Our results strongly suggest that the enzymatic adaptation of the HIV-1 RT DNA polymerase active site to catalyze DNA synthesis in cellular environments that contain low levels of dNTPs is a major contributor to the unique ability of these viruses to efficiently replicate in macrophages. Therefore, this study provides evidence that RT plays an essential role in establishing and maintaining the macrophage tropism of HIV-1 during the course of viral infection, which presents unique virological and pathological characteristics that differentiate lentiviruses from oncoretroviruses.

## REFERENCES

- Traut, T. W. (1994) *Mol. Cell. Biochem.* **140**, 1–22
- Angus, S. P., Wheeler, L. J., Ranmal, S. A., Zhang, X., Markey, M. P., Mathews, C. K., and Knudsen, E. S. (2002) *J. Biol. Chem.* **277**, 44376–44384
- Jackson, R. C., Lui, M. S., Boritzki, T. J., Morris, H. P., and Weber, G. (1980) *Cancer Res.* **40**, 1286–1291
- Hauschka, P. V. (1973) *Methods Cell Biol.* **7**, 361–462
- Fuller, S. A., Hutton, J. J., Meier, J., and Coleman, M. S. (1982) *Biochem. J.* **206**, 131–138
- Skoog, L., and Bjursell, G. (1974) *J. Biol. Chem.* **249**, 6434–6438
- Zhao, X., Chabes, A., Domkin, V., Thelander, L., and Rothstein, R. (2001) *EMBO J.* **20**, 3544–3553
- Chabes, A., Georgieva, B., Domkin, V., Zhao, X., Rothstein, R., and Thelander, L. (2003) *Cell* **112**, 391–401
- Yao, R., Zhang, Z., An, X., Bucci, B., Perlstein, D. L., Stubbe, J., and Huang, M. (2003) *Proc. Natl. Acad. Sci. U. S. A.* **100**, 6628–6633
- Zhao, X., and Rothstein, R. (2002) *Proc. Natl. Acad. Sci. U. S. A.* **99**, 3746–3751
- Lewis, P. F., and Emerman, M. (1994) *J. Virol.* **68**, 510–516
- Lewis, P., Hensel, M., and Emerman, M. (1992) *EMBO J.* **11**, 3053–3058
- Kim, B. (1997) *Methods (Orlando)* **12**, 318–324
- Weiss, K. K., Chen, R., Skasko, M., Reynolds, H. M., Lee, K., Bambara, R. A., Mansky, L. M., and Kim, B. (2004) *Biochemistry* **43**, 4490–4500
- Diamond, T. L., Kimata, J., and Kim, B. (2001) *J. Biol. Chem.* **276**, 23624–23631
- Malboeuf, C. M., Isaacs, S. J., Tran, N. H., and Kim, B. (2001) *BioTechniques* **30**, 1074–1078, 1080, 1082
- Weiss, K. K., Bambara, R. A., and Kim, B. (2002) *J. Biol. Chem.* **277**, 22662–22669
- Diamond, T. L., Souroullas, G., Weiss, K. K., Lee, K. Y., Bambara, R. A., Dewhurst, S., and Kim, B. (2003) *J. Biol. Chem.* **278**, 29913–29924
- Balakrishnan, M., Roques, B. P., Fay, P. J., and Bambara, R. A. (2003) *J. Virol.* **77**, 4710–4721
- Boosalis, M. S., Petruska, J., and Goodman, M. F. (1987) *J. Biol. Chem.* **262**, 14689–14696
- Roy, B., Beuneu, C., Roux, P., Buc, H., Lemaire, G., and Lepoivre, M. (1999) *Anal. Biochem.* **269**, 403–409
- Klimatcheva, E., Planelles, V., Day, S. L., Fulreader, F., Renda, M. J., and Rosenblatt, J. (2001) *Mol. Ther.* **3**, 928–939
- Akkina, R. K., Walton, R. M., Chen, M. L., Li, Q. X., Planelles, V., and Chen, I. S. (1996) *J. Virol.* **70**, 2581–2585
- Maddon, P. J., Dalgleish, A. G., McDougal, J. S., Clapham, P. R., Weiss, R. A., and Axel, R. (1986) *Cell* **47**, 333–348
- Maybaum, J., Klein, F. K., and Sadee, W. (1980) *J. Chromatogr.* **188**, 149–158
- Huang, D., Zhang, Y., and Chen, X. (2003) *J. Chromatogr. B Analyt. Technol. Biomed. Life Sci.* **784**, 101–109
- Decosterd, L. A., Cottin, E., Chen, X., Lejeune, F., Mirimanoff, R. O., Biollaz, J., and Coucke, P. A. (1999) *Anal. Biochem.* **270**, 59–68
- Di Piero, D., Tavazzi, B., Perno, C. F., Bartolini, M., Balestra, E., Calio, R., Giardina, B., and Lazzarino, G. (1995) *Anal. Biochem.* **231**, 407–412
- Kaushik, N., Talele, T. T., Pandey, P. K., Harris, D., Yadav, P. N., and Pandey, V. N. (2000) *Biochemistry* **39**, 2912–2920
- Preston, B. D., Poiesz, B. J., and Loeb, L. A. (1988) *Science* **242**, 1168–1171
- Roberts, J. D., Preston, B. D., Johnston, L. A., Soni, A., Loeb, L. A., and Kunkel, T. A. (1989) *Mol. Cell. Biol.* **9**, 469–476
- Menendez-Arias, L. (1998) *Biochemistry* **37**, 16636–16644
- Gutierrez-Rivas, M., Ibanez, A., Martinez, M. A., Domingo, E., and Menendez-Arias, L. (1999) *J. Mol. Biol.* **290**, 615–625
- DeFife, K. M., Jenney, C. R., Colton, E., and Anderson, J. M. (1999) *J. Histochem. Cytochem.* **47**, 65–74
- Krombach, F., Munzing, S., Allmeling, A. M., Gerlach, J. T., Behr, J., and Dorger, M. (1997) *Environ. Health Perspect.* **105**, 1261–1263
- Munch-Petersen, B., Tyrsted, G., and Dupont, B. (1973) *Exp. Cell Res.* **79**, 249–256
- Kinter, A., Arthos, J., Cicala, C., and Fauci, A. S. (2000) *Immunol. Rev.* **177**, 88–98
- Moore, J. P., Trkola, A., and Dragic, T. (1997) *Curr. Opin. Immunol.* **9**, 551–562
- Durban, E. M., and Boettiger, D. (1981) *Proc. Natl. Acad. Sci. U. S. A.* **78**, 3600–3604
- Durban, E. M., and Boettiger, D. (1981) *J. Virol.* **37**, 488–492